INCLUSION DETECTION IN MOLTEN ALUMINUM: CURRENT ART AND NEW AVENUES FOR IN SITU ANALYSIS

Shaymus W. Hudson and Diran Apelian
Advanced Casting Research Center, Worcester Polytechnic Institute, 100 Institute Road, Worcester, MA 01609, USA

DOI 10.1007/s40962-016-0030-x

Abstract

In order for light metals to meet the demands for critical applications in the automotive and aerospace industries, tight control over the composition and cleanliness of the metal must be achieved before casting. Melt cleanliness manifests primarily in the amount of inclusions present. A review of the state of the art in detecting and quantifying solid particle inclusions is given. Quick analysis of melt composition and quality, carried out in situ, is of great value in casting operations. Such quick measurements in the liquid alleviate analyzing samples in the solid state and thus increase productivity. The use of laser-induced breakdown spectroscopy as a new tool for quantifying melt cleanliness in situ is discussed.

Keywords: *inclusions, cleanliness, oxides, quality*

Introduction

Light metals, aluminum and its alloys in particular, have been the source of significant interest as materials for structural applications for the automotive, aerospace, and defense industries. The appeal of aluminum comes from its high specific strength, thermal conductivity, and corrosion resistance, which translate to reduction in vehicle weight and fuel consumption.[1,2] In order for light metals to continue to replace ferrous metals for such applications, proper preparation of the molten alloy prior to casting or extrusion is essential. This entails control over the chemical composition and, more importantly, its cleanliness.

In general, the cleanliness of aluminum alloys primarily refers to the concentration of solid particle inclusions (exogenous and intrinsic), dissolved hydrogen, and residual elements to a lesser extent.[3] When the quantity of any of these detractors exceeds a certain threshold limit, dictated by the intended use of the product, they will lead to unacceptable performance and early failure. Inclusions have a significant influence on the properties of aluminum. It has been shown that inclusion-rich metal results in lower metal fluidity and feeding capability during casting, lower mechanical properties, increased scrap rate, decreased machinability, and poor surface finish. There are several sources of these impurities, including the electrolysis process during primary aluminum production, surface turbulence, pouring atmosphere, and the interactions between the molten metal with alloying elements and refractory materials. Melt quality can be controlled by the removal of these elements and particles. Therefore, various technologies have been developed over the past 40 years to measure and remove these impurities.

The application of inclusion reduction techniques during casting can help limit the size and amount of inclusions remaining in the molten metal and its products. Such advances include rotary degassing and fluxing as well as ceramic foam and deep bed filtration. Advances in counter-gravity casting and modeling have allowed for optimized casting processes with minimal surface turbulence. Nonetheless, the difficulty of quantifying cleanliness, differentiating "clean" from "really clean" metal, has still not been fully realized. Chemistry, concentration, and size distribution of inclusions are particularly important to producers of clean metal. Depending on the application, an inclusion of 5–10 microns may be insignificant or the root cause of a rejected casting.

This paper will review and compare current techniques and methods of detecting and quantifying solid particle inclusions. It will also discuss experimental techniques that could be used to achieve the goal of in situ monitoring of inclusion content.

Inclusion Sources

Inclusions are defined as any exogenous solid- or liquid-phase particles present above the liquidus temperature of the molten metal matrix. Many kinds of inclusions can be present in the melt, including furnace dross, salts, and unmelted elements. The amount of unwanted particles in molten metal can be substantial. As can be seen in Figure 1, a small concentration of inclusions can yield a high number count. For example, 1 ppm of 40-micron inclusions results in 4000 particles in one kilogram of metal. Such particles can be exogenous or form in situ as seen in Table 1. They can be further characterized by their composition, size distribution, morphology, and phase (Figure 2). The number of inclusions present depends on a number of factors, including initial melt composition, solidification rate, and pouring atmosphere.[4–9]

The most common inclusions in aluminum are oxide particles and films. They are most commonly formed by direct oxidation in air or by reaction with water vapor:

$$2Al + \frac{3}{2}O_2 \rightarrow Al_2O_3 \qquad \text{Eqn. 1}$$

$$2Al + 3H_2O \leftrightarrow 3H_2 + Al_2O_3 \qquad \text{Eqn. 2}$$

Oxides can also form via alumino-thermic reactions with oxides of other metals, such as iron or silicon, contained in tools and refractories. Aluminum and its alloys oxidize readily in both the solid and molten states to provide a continuous self-limiting film. The rate of oxidation increases with temperature and is substantially greater in molten than in solid aluminum. The reactive elements contained in aluminum alloys such as magnesium, strontium, sodium, calcium, beryllium, and titanium are also factors in oxide formation. In both the molten and solid states, the oxide formed at the surface offers benefits in self-limitation of further oxide growth. It also acts as a barrier to hydrogen diffusion, another melt quality detractor. However, the low viscosity of liquid aluminum allows for induced turbulence either by handling or pouring. Surface turbulence results in the entrainment of oxide particles and films.[5] Al_2O_3 films can also include oxides such as SiO_2, $MgAl_2O_4$, MgO, and others depending on the alloy.[11] Although oxide inclusions can sink, they often rise too and remain at the melt surface.[9] The high surface-to-volume ratio and poor wettability of oxide films in Al act as driving forces for inclusions to remain close to a free surface as well as cause their agglomeration.[12]

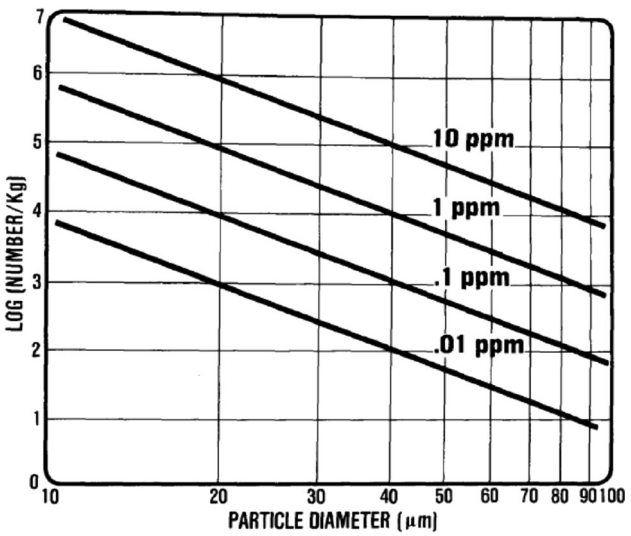

Figure 1. Relationship between inclusion concentration (number/kg) and particle diameter for varying concentrations.[10]

Spinel inclusions arise from melting scrap as well as the addition of magnesium to the holding furnace. MgO, due to its lower free energy of formation compared to Al_2O_3, tends to form preferentially in alloys with more than 0.5 wt% Mg. In addition, adding low purity Mg can create spinels and non-metallics such as MgS and MgF_2.[13]

Silicates can originate from the erosion of ceramic materials (used in the melting operation) as well as dissolved Si reacting with the atmosphere. Refractory particles can agglomerate and form complex oxides like $Al_2O_3{\cdot}SiO_2{\cdot}CaO$.[14] Carbides such as SiC and Al_4C_3 often come from pyrolyzed hydrocarbons in recycled aluminum melts as well as residual coolants and oils in recycled machining chips and pot cells primary in Al smelting.[9] Nitrides can come from overly degassing with nitrogen gas as well as the addition of magnesium as an alloying element. Mg_3N_2 inclusions in the magnesium can react with the aluminum to form AlN. Other particles such as MgF_2 and MgS can appear in Al from sub-par magnesium.[15]

Intermetallic compounds can arise from a variety of sources including residual elements (from smelting, melting and remelting), alloying, and grain refining. For example, grain refiners like TiB_2 and dissolved elements, such as Fe and Ni, can create unwanted aluminides and borides. Precipitation of such phases is often only found in die casting, where processing temperatures are lower than the melting points of many intermetallics.[8,16,17]

Liquid-phase inclusions can also form in molten aluminum due to fluxing or chlorinating. They are often in the form of molten salts ($CaCl_2$, NaCl, $MgCl_2$, and KCl) and can also contain fine fluoride particles (NaF, AlF_3, and CaF_2).[18,19]

Effect of Inclusions on Properties

Solid inclusions remaining in the metal can result in a plethora of product defects. Inclusions reduce mechanical properties by acting as stress concentrators and allow for cracks to form at their interfaces. This can lead to rapid crack propagation, large crack paths, and ultimately early failure. Properties such as elongation, yield stress, and fracture toughness have been observed to decrease when a

Table 1. Inclusions Observed in Aluminum Alloys[1,4,6–8,14,16–19]

Phase	Morphology	Size range (μm)	Impurity elements also commonly present
Oxides			
$MgAl_2O_4$ (spinel)	Particles, films	0.1–5000	N, Na, K, Ca, Si, Zn and/or Fe
Al_2O_3 (corundum)	Particles, films	0.1–5000	N, Na, Mg, Si, Zn, Fe, Ca, K, Cl and/or F
MgO	Particles, films	0.1–5000	–
SiO_2	Particles, clusters	0.5–30	K, Ca, Na and/or Al
CaO	Particles	<5	–
Calcium silicates (Ca, Si, O)	Particles, clusters	10–100	K, Na
Potassium silicates (K, Si, O)	Particles, clusters	10–1000	Na, Ca, Al, Mg and/or Ti
Carbides			
Al_4C_3	Particles, clusters	0.5–25	–
Al_4O_4C	Particles, clusters	0.5–25	–
SiC	Particles	0.5–5	–
Nitrides			
AlN	Particles, films	10–50	–
Borides			
TiB_2	Particles, clusters	1–30	V, Zr, and/or Cr
AlB_2	Particles	0.1–3	–
Others			
Chlorides and salts ($CaCl_2$, NaCl, $MgCl_2$)	Liquid droplets	0.5–1	–
Ultrafine gas bubbles (Ar, N_2)			
Intermetallics ($TiAl_3$, TiAl, NiAl, Ni_3Al, etc.)	Particles, rods, clusters	10–100	–

high percentage of inclusions is observed on the fracture surface. An inclusion contributing to 1 % of the fracture area can cut elongation in half.[20–22] Fatigue properties are also severely affected by the presence of inclusions. Because they tend to act as crack initiators, fatigue life curves typically decrease as inclusion content increases. In addition, small inclusions, too small to act as crack initiators, will contribute to fatigue crack propagation.[23] In addition to being crack initiation sites, oxide inclusions can act as heterogeneous nucleation sites for hydrogen pores. This promotes voids and hydrogen porosity, further reducing static and dynamic properties.[24,25] With regard to other properties, it has been well documented that inclusions can negatively influence melt fluidity,[26,27] as well as the machinability and surface finish of castings. In production of aluminum sheet and foil, inclusions have been known to cause holes and tears.[28]

Cleanliness Measurement Methods

Metallography

Traditional metallography involves the physical examination of ingot slices to determine the presence and type of inclusions. The sample is cut, polished, and microscopically examined. The prepared surface can then be analyzed in a variety of ways. Published standard comparisons exist, but typically only for steels.[29] This is mainly due to the extremely low volume fraction of inclusions in aluminum preventing the ability to differentiate between clean and very clean metal. Charts also, at most, provide a semi-quantitative measure of melt cleanliness.

The use of software-based image analysis systems makes it possible to obtain quantitative analyses of inclusions. Provided the image processor has a high enough resolution, image analysis can quantify spatial distribution and clustering of inclusions in addition to size distribution and area fraction.[30] There is a variety of statistical analyses that can be performed to characterize features of inclusions.

Once scanned, the number of inclusions per unit area can be counted. The degree of clustering of the particles can be described by the standard deviation:

$$\sigma = \sqrt{\left(\frac{1}{n}\right)^2 \sum \left(N_A - \overline{N_A}\right)^2} \qquad \text{Eqn. 3}$$

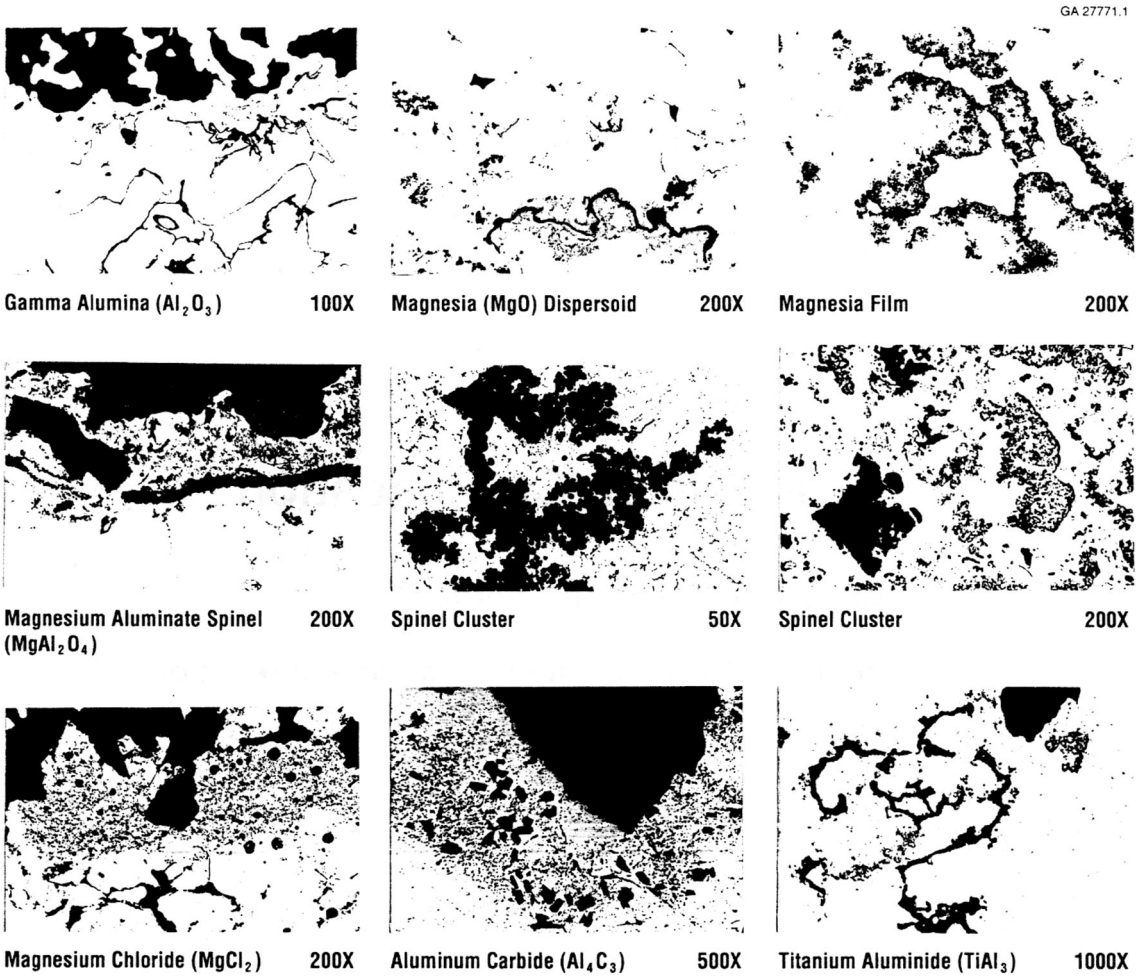

Figure 2. Micrographs of typical inclusions in aluminum castings.[1]

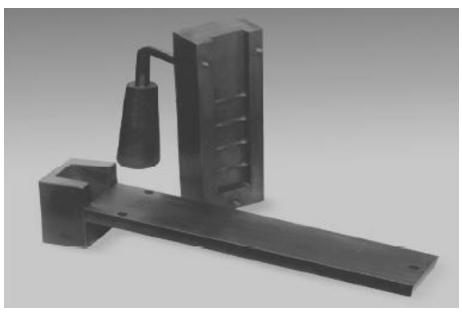

Figure 3. A K-mold apparatus.[34]

where "N_A" is the observed number of particles per unit area in a given field of view and "N_A" bar is the average number of inclusions per unit area in "n" fields of view on the sample. If the inclusions are evenly distributed, the standard deviation is small. If there is significant clustering, standard deviation increases. To compare samples with different concentrations or number densities, the coefficient of variation (σ normalized by N_A bar) should be used.

Area fraction can also be easily found by image analysis. Similar to number density calculations, the standard deviation and coefficient of variation for area fraction can be determined. If the special distribution of particles is homogeneous, then σ and the coefficient of variation are small. Nearest neighbor subdivision of the sample surface into a grid, or creating a Dirichlet tessellation, can analyze spacing and spatial distribution.[31]

In addition to physical characteristics of inclusions, each particle can be analyzed chemically via energy-dispersive spectroscopy (EDS) in an electron microscope. The combination of particle chemistry, concentration, and size distribution allows for a complete understanding of the inclusions present in a casting process.

Metallography of melt samples can give an excellent view into the nature of inclusions present, but it is limited in several ways. Because samples need to be taken from the melt, and because preparing and analyzing each sample requires some time, this method only yields a small sample size. Although image software and other tools exist to

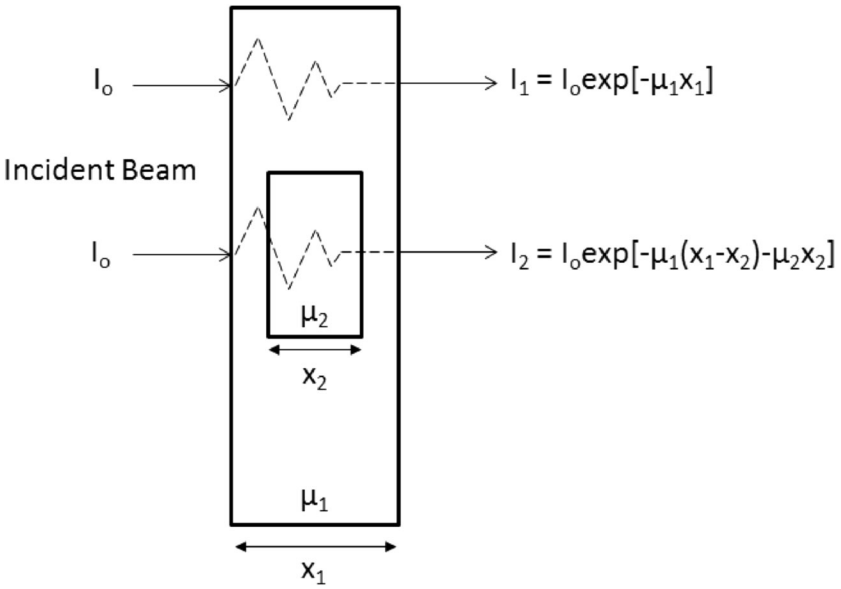

Figure 4. Schematic of the X-ray transmission process. The differences between I_1 and I_2 result in contrast between two phases.[35]

make analysis easier, there is still a delay between taking the sample and obtaining results. In addition to time, metallography only looks at a cross section of the sample. The small amount of metal that can be analyzed cannot be fully representative of a large casting. The size and morphology of inclusions present cannot be fully realized because only a small area is examined, forcing researchers and technicians to quantify the amount by square millimeter of inclusions per kilogram of melt.[32] Nonetheless, certain facets of the size distribution of particles in the bulk melt can be predicted. The methods of predicting the largest inclusion in a large volume of metal is well described and documented in a review paper on clean steels by Atkinson and Shi. Such methods include extrapolation of the size distribution function, statistics of extremes, and generalized Pareto distributions.[23]

K-mold

Metal cleanliness has often been assessed by determining their mechanical properties; hence, fracture tests have also been used for inclusion assessment. The most well-known fracture test for aluminum is the K-mold test, invented by Sanji Kitaoka at the Nippon Light Metal Ltd in 1973.[33] Liquid aluminum (approx. 400 g) is poured into the mold and produces a small casting consisting of a flat plate with four notches that acts as fracture points. A K-mold apparatus is seen in Figure 3.

The K-mold test involves casting one or more of these notched plates. The plate is then broken at each notch. The surfaces are examined either by eye or a microscope. The presence of large inclusions or inclusion clusters will induce failure. Oxides are readily detected on the fracture surface due to their visual difference in contrast compared to the fine aluminum matrix produced by rapid solidification in the K-mold.

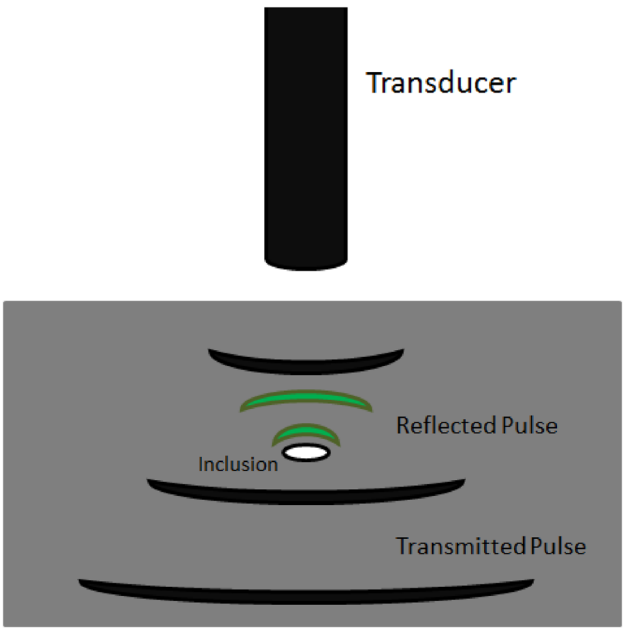

Figure 5. A schematic of the basic principles of ultrasound. An inhomogeneity, such as an inclusion, will reflect the transmitted pulse back to the surface.

The cleanliness level of different pots can be evaluated by comparing the number and size of inclusions on the fracture surface. The visual observation of inclusions on the fracture surface is used to determine a *K* value for the batch and compared to a preset standard. This value is calculated as:

Figure 6. Porous disk filtration apparatus.[51]

$$K = \frac{s}{n} \qquad \text{Eqn. 4}$$

where "K" is the K-mold value, "n" is the number of examined samples, and "s" is the total number of inclusions found in n pieces.[33]

The main advantage of a K-mold is that it allows for easy characterization of the larger inclusions and is good for real-time testing of macroscopic defects (coarse inclusions, gross oxides, and gas bubbles). However, the volume tested is a small part of the bulk and the statistical evaluation of the results is difficult. As a result, this method is not as sensitive for very clean melts and is accurate only for large inclusions.

X-ray Radiography

X-ray radiography is a standard non-destructive technique for determining casting quality. In addition to detecting inclusions and pores, radiography is used to find other flaws such as internal cracks, shrinkage, confluence welds, and hot tears. Radiographs of a sample (or the entire cast part) are analyzed with respect to standardized images (ASTM E155-10). The basic operating principle of radiography involves how certain solid phases absorb X-rays differently. As an X-ray travels through matter, the way it interacts with the material depends on the material's refractive properties. An example schematic displaying the concept is seen in Figure 4. If two phases are present in the material analyzed, there will be a difference in attenuation leading to image contrast.

Although radiographs allow for detection of inclusions as well as morphology and relative position in castings, it is limited by its inability to generate three-dimensional images and determine particle chemistry. The process is also lengthy and is typically used to analyze parts once they have been cast. Even then, there are limitations with respect to casting thickness. The ability of X-rays to transmit through metal is a function of its thickness. Thick sections of castings cannot be fully interrogated, unless high-energy X-ray sources are used. As a result, only defects larger than 50–100 microns can be detected unless microradiography on small, thin samples is used.[36]

X-ray Tomography

X-ray tomography (XRT) is a more advanced use of X-rays. First used for medical applications, 3D visualization of microstructures by XRT has been successfully performed for many other metallurgical studies, such as Pb-free solder joints, powder metallurgy steels, and metal matrix composites. By analyzing radiographs taken around a single axis of rotation, cross-sectioning images can be compiled to create a 3D image. This eliminates cross-sectioning and allows for superior resolution and image quality with minimal sample preparation. This method requires high-energy, monochromatic X-rays to form the 3D composite image.

Images generated can have a similar resolution to that seen in metallographic samples. Since the sample does not have to be cut and polished, analysis time can be reduced. With proper imaging software, the morphology, size distribution, position, and volume fraction of inclusions can be accurately determined within the sample.[37–39] Because different phases will have different X-ray absorption coefficients, chemistry of inclusions can be determined in principle. However, in practice, the small difference between X-ray absorbance coefficients of most oxides prevents XRT from being used as a reliable method for inclusion identification. One drawback to tomography is the small sample size (similar to metallography). Even with a decreased sample preparation time, many samples must be taken to get meaningful statistics on cleanliness in the bulk melt. Another drawback is the cost of tomography; at present, it is more of a laboratory-based detection method.

Ultrasound

Ultrasound has been widely used to probe substances via pulsed sound waves. Once such technique used for microanalysis is scanning acoustic microscopy (SAM).[40] Similar to sonar, a sound pulse is generated by a transducer toward the sample surface. The pulse then propagates into the bulk of the sample. When the pulse encounters a feature (like the inclusion in Figure 5), a portion of the pulse is reflected back. The reflected signal, read by the transducer, will contain a transient peak whose magnitude will correspond to the size and shape of the feature. The probe scans over the entire sample area to generate the acoustic image. Depending on the mechanical and acoustic properties of the matrix and internal features, certain amplitudes will be

reflected. This allows SAM to detect features such as phase and grain boundaries, voids, pores, cracks, and inclusions.

For solid materials, sound pulses in the MHz and GHz range are used. In a study on 319 aluminum by Meav et al., microstructural features such as eutectic Si, shrinkage porosity, and dendrite arms were observed. For resolution on the order of 50–100 microns, only a penetration depth of a few millimeters was possible.[38] Although SAM has a resolution comparable to optical microscopy without the need for sample preparation, the fact that penetration is limited depending on the desired resolution is the main drawback for this technique.

The same principles can be applied to molten metal. In situ ultrasound has been explored as early as the 1960s by Pitcher and Young and was further developed by Alcan, Alcoa, and Reynolds Aluminum throughout the 1980s.[10,41–43] More recently, using research by Mountford and Sommerville at the University of Toronto, an ultrasonic probe to detect and measure inclusions in liquid metal was developed by Metalvision Manufacturing Canada Ltd.[44] The probe, marketed as the MV20/20, has separate transducers to emit and collect sound waves. The transmitter pulses at a rate of 100 Hz allows for thousands of measurements to be taken in minutes. Because the transmitter and receiver are at an angle to each other, there is an effective sensing zone within the molten metal. This size of this region is not reported in the literature. Metalvision produces portable models and systems that can be integrated for crucibles or a launder system. The MV20/20 outputs three pieces of information: (1) largest particle size, (2) number of particles, and (3) a qualitative cleanliness value. The amplitudes of the reflections from particles in the metal determine inclusion size. However, the machine can only detect particles between 20 and 160 μm due to factors such as signal to noise and the slow degradation of the probe materials. The number count of inclusions is given per 1000 measurements. In a comparative industrial trail reported by Metalvision, the MV20/20 cleanliness values correlate well with PoDFA results.[45,46]

Filtration Methods

Pressure filtration works by forcing a molten aluminum sample under pressure through a fine filter, which traps inclusions. The inclusions are concentrated 5000–10,000 times on the filter surface, which can then be analyzed metallographically. Although samples taken from the melt are relatively small (1–2 kg), concentration of inclusions offers reliable, industrially accepted results.[47] There are several industrial measurement devices that are all based upon this principle, including PoDFA, LAIS, Prefil Footprinter, and Qualiflash; these are reviewed below.

PodFA

The porous disk filtration analyzer (PodFA) (Figure 6), manufactured by ABB Inc., is a shop floor technique in which 2 kg of melt is ladled into a preheated crucible. The unit draws the molten sample through a small ceramic filter using a vacuum; this traps the inclusions for later analysis. The test is stopped when approximately 1.5 kg of the metal has been filtered. Since the filter disk must be sliced for study, the concentrations of inclusions are given in mm^2/kg

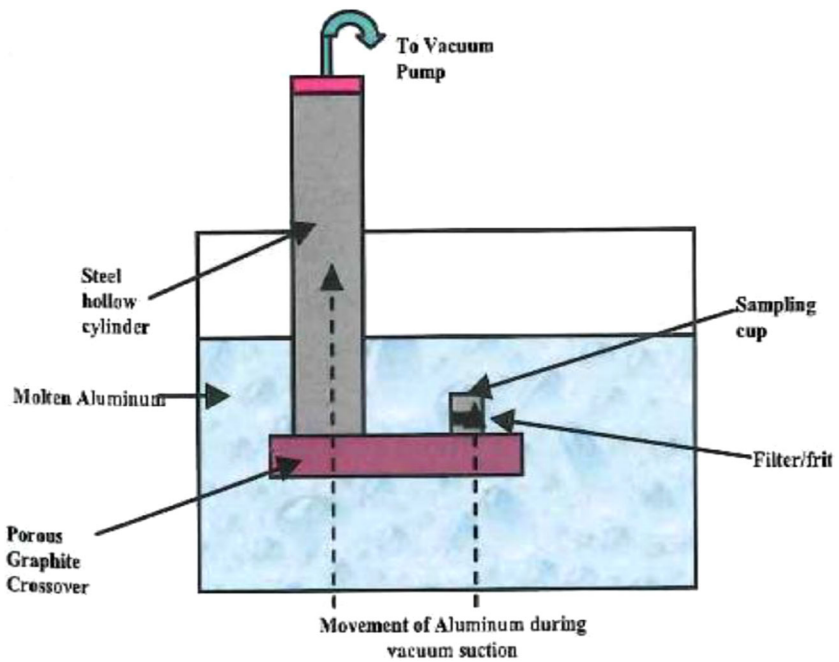

Figure 7. Schematic of a LAIS apparatus.[18]

of melt. A number count of inclusions per kg of metal can also be tabulated. A curve generated during this test shows the filtration rate, which can also be used as cleanliness metric with PodFA.[48] Metallographic analysis results in a classification of inclusions (MgO, spinels, borides, carbides, etc.).

Although this test is inexpensive to set up, it has several disadvantages. Samples are time-consuming to gather and expensive to analyze. Results will not be available for at least 24 h and can take up to 5 days. As a result, PoDFA is often used to optimize a process and/or to distinguish very dirty metal (>1 mm^2/kg) and relatively clean metal (<1 mm^2/kg).[32,48]

LAIS

The liquid aluminum inclusion sampler (LAIS), developed by Union Carbide, is similar to PodFA but with a more direct sampling method.[49,50] As seen in Figure 7, the apparatus is submerged within the melt. The molten metal is then pumped through a sampling cup with ceramic frit. Once the steel tube to the vacuum pump is filled, the assembly is placed on a chill block to allow for unidirectional cooling. A typical LAIS sample is a 1.7 in. by 0.7 in. cylinder. Once removed, it is then microscopically analyzed. Like PodFA, the units for inclusion content are mm^2/kg.[51] The advantage of this procedure is that it samples directly in the melt and can be manipulated to take measurements at different depths and locations.

Prefil Footprinter

The Prefil Footprinter, like PoDFA and LAIS, forces a melt sample through a small filter (Figure 8a). It then measures the flow rate as a metric for metal quality. A fixed volume of metal is poured into the test crucible and filtered at approximately 10–12 psi. A load cell in the collector mold determines the mass flowing through as a function of time (Figure 8b). The shape of the curve is dependent on the mixture of inclusions present. Very clean metal flows quickly giving a steep, straight line in the output graph. The software allows the fluidity curve generated to be compared with previous data and standards developed by the manufacturer. If necessary, the filter can be examined metallographically.[18] Although the Prefil gives a quick readout, it is highly dependent on sampling technique of the user, melt temperature, and gives only a semiquantitative view of melt cleanliness. Concentration and size distribution cannot be directly determined from a flow rate curve.

Qualiflash

The Qualiflash technique, like Prefil, uses the mass of metal passing through a filter as a means of assessing cleanliness (Figure 9a). A fixed volume of melt is filtered through a ceramic disk and poured into a 10-stepped ingot mold. The dirtier the melt, the fewer steps filled. The end result is a cleanliness rating based on the number of steps filled known as the *Q* level (Figure 9b).[34] Like the Prefil, it yields a quick result, but is highly dependent on sampling technique, melt temperature, and gives only a semiquantitative measurements.

Centrifugation

Using a hot centrifuge to analyze particles in metals has been used as early as the 1950s. By taking advantage of the differences in density between inclusions and the metal matrix, the particles can be concentrated and analyzed similarly to pressure filtration techniques. As derived by

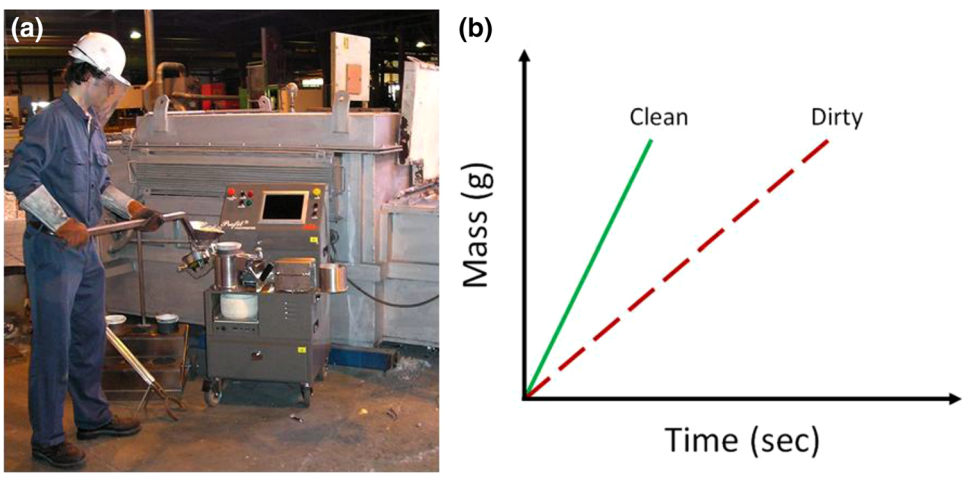

Figure 8. (a) A Prefil Footprinter in use; (b) Example of data from a Prefil Footprinter.[34]

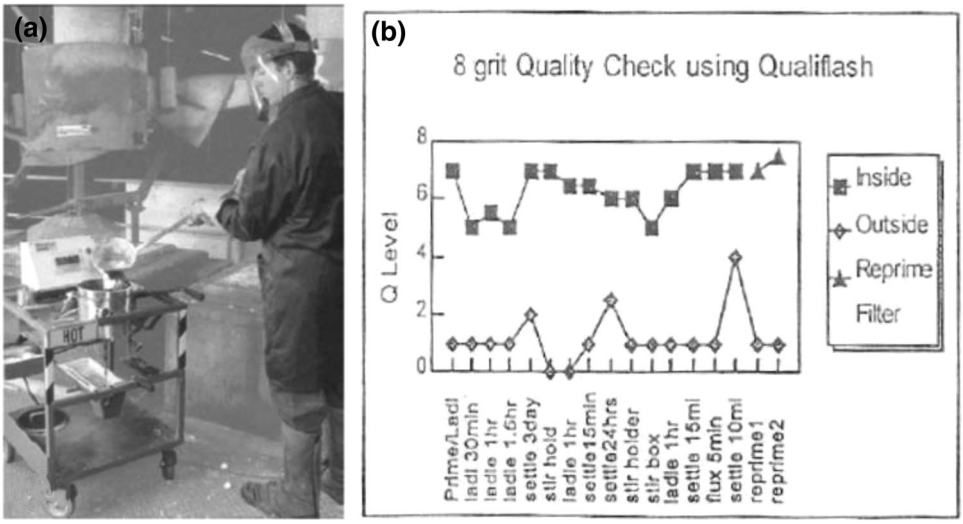

Figure 9. (a) A Qualiflash apparatus in use; (b) An example of data gained from Qualiflash.[36]

Siemensen, the smallest possible particle to reach the bottom of the spinning crucible has a defined size:

$$d = \left[\frac{45\eta_l \ln\left(\frac{r_B}{r_T}\right)}{8g^2\alpha \times f^2(\rho_p - \rho_M)\left(t - \frac{7}{12}\tau\right)}\right]^{1/2} \quad \text{Eqn. 5}$$

where η—viscosity coefficient of the liquid at time $t \approx 0.2(T(t) - T_M)^{-0.25}$, r_B—distance between the axis of rotation and the bottom of the melt, r_T—distance between the axis of rotation and the top of the melt, g—gravitational acceleration, α—relative speed of the particle to that of a sphere with the same volume, f—rotational frequency, ρ_P—density of a particle, ρ_M—density of the melt, t—time, τ—time to reach rotational frequency f.

Siemensen found, in centrifuge experiments on molten aluminum, inclusions down to 0.5 μm could be forced to the bottom of the crucible. In addition to inclusions, both stable and unstable intermetallics are also forced to the bottom and can be analyzed using standard metallographic techniques.[16] Although centrifugation is a relatively simple way to concentrate inclusions, the sample size is quite small. Experiments using this technique have analyzed samples ranging from 100 to 200 g.[16,52]

Electrochemical Dissolution

The use of acid etchants has been used extensively in metallography to dissolve the matrix and retain intermetallic and other secondary phases. The same approach can be used to analyze inclusions by using a strong acid (HCl, HF, or HNO_3) to completely dissolve the metal matrix. The oxides will, in principle, not dissolve. The particles remaining in solution can be analyzed by a Coulter counter.[17] Particles can then be filtered out and analyzed on the microscope or by X-ray diffraction.[53] However, complete dissolution is quite lengthy. Siemensen found that it took approximately 7 min to dissolve 20 g of Al–5 %Ti–1 %B at room temperature using a 20 % HCl solution. Assuming the dissolution rate is constant, it would take approximately 6 h to dissolve 1 kg of the same metal. In addition, undissolved and partially dissolved intermetallics as well as surface oxides will skew particle size results in the Coulter counter. Because of the time required and delicate nature of this method, it can only be performed in the laboratory.

Electrical Resistivity

Another method that is common in the metals processing field is the use of electrical resistivity to sense inclusions, similar to that of a Coulter counter for aqueous solutions. In work done by Doutre and Guthrie in the 1970s and 1980s, technology was developed that allowed molten aluminum to be drawn through a small aperture in the presence of a large DC current. Because inclusions are nonconductive, the resistances through the aperture increases as particles pass through. Because the voltage measurements taken are proportional to the size of the inclusions, and that the amount of liquid drawn through could be quantified, a real-time volumetric distribution of particles could be measured.[54] A schematic of this process can be seen in Figure 15. The LiMCA (liquid metal cleanliness analyzer), marketed by ABB Inc. and currently on its third generation, is the most widely used embodiment of this technique.[28]

The LiMCA probe consists of a quartz tube with a small orifice approximately 300 μm in size. As show in Figure 10, electrodes are placed inside and outside the tube. Liquid metal is drawn through the orifice to collect data. A typical sample volume is approximately 7.5 mL (17.5 g). The length of the tube is fixed, and therefore, the sampling

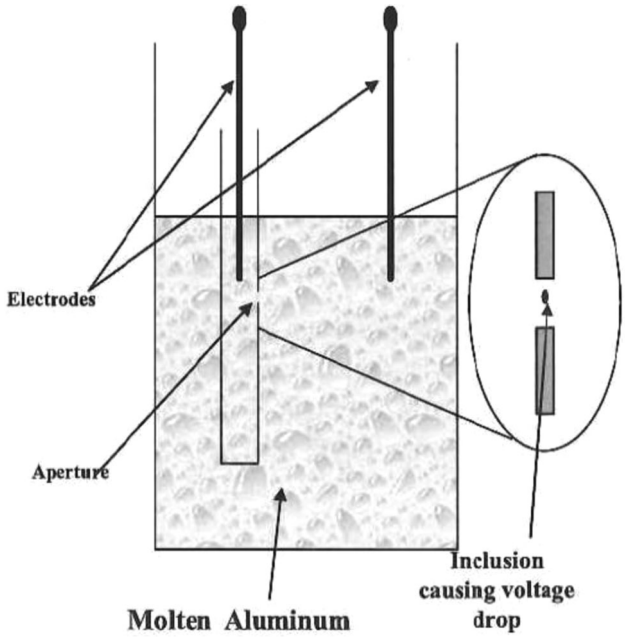

Figure 10. Schematic of a LiMCA apparatus.[56]

position is fixed. However, longer quartz tubes, allowing for deeper sampling, have been developed for experimental purposes.[55]

The resolution of LiMCA is limited by the background electrical noise and the orifice diameter. In general, LiMCA can theoretically capture particles between 20 and 300 μm. In practice, a particle range of 20–100 μm is more common as orifice holes may become easily blocked.[18] It has been estimated that as many as 60 % of the total inclusions in a given melt may remain undetected.[57]

Reduced Pressure Test

The reduced pressure test (RPT) provides qualitative and semiquantitative information of overall melt cleanliness. A molten sample of 100–200 g is solidified under a reduced pressure of 26 mmHg. As a result, formation and growth of hydrogen pores is significantly enhanced because of the decrease in hydrogen solubility with respect to pressure.[37] The solidified sample can be analyzed in a number of ways. The most qualitative method is to section the RPT sample in half and examine the cut surface for pores. Another common method is to measure the sample's density.

If one assumes that a certain fraction of inclusions can be nucleated on or concentrated by the gas pores, then the RPT may also be able to qualitatively provide information on melt cleanliness. Visual comparison charts are used to give an estimate of the overall melt cleanliness. A low number of pores imply a cleaner melt. However, RPT measurements are highly sensitive to many variables, including sampling turbulence, chamber vacuum pressure,

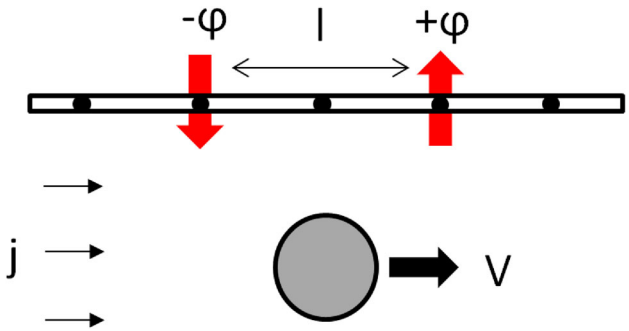

Figure 11. Schematic of Makarov's voltage probe. The gray particle induces a positive and negative potential across the probe array. The distance l is related to the size of the inclusion.

vibration, and solidification rate.[58] Work has been performed on developing a statistically optimized procedure to increase data reliability. It was found that turbulence during sampling had the largest variation in results.[59]

Multiple Voltage Probe Sensors

In the early 2000s, Makarov et al., developed a sampling scheme to detect inclusions in liquid aluminum via a voltage probe array (Figure 11). They proposed a sensor that consisted of a flat plate with evenly spaced voltage electrodes. By applying an electric current through the conductive aluminum, the non-conductive inclusion could be mapped by the probe array.[60]

If an inclusion passes by the array, two peaks would appear on the sensor, one the inverse of the other. It was found that the voltage peak magnitude, "$\phi'_{\max}$", is related to particle radius "r" by the relation:

$$\varphi'_{\max} = \frac{4}{3\sqrt{3}} \frac{jr^3}{\sigma l^2} \qquad \text{Eqn. 6}$$

Here, "l" is the distance between peaks on the voltage sensor, "j" is the applied current density through the molten metal, and "σ" is the electrical conductivity of the metal.[60]

It was found that the experimental sensor could detect inclusions from 100 to 1000 μm in size.[60] Although it may not achieve the same sensitivity as a Coulter counter system, a voltage probe may be less expensive to implement since it does not require an aperture or vacuum pump to draw in liquid for sampling.

Electromagnetic/Optical Sensing

Also proposed by Makarov et al., was a method to concentrate inclusions to a free surface through Lorenz forces. By applying a DC current between two electrodes in a

Table 2. Comparison of Measurement Techniques[10,16–18,23,32–34,42,59,62–64]

Method	Test locale	Estimated analysis time	Estimated sample size	Measurement unit	Inclusion size?	Chemistry?
Metallography	Laboratory	4–10 h	5–20 g	mm^2/kg	Yes	Yes
K-mold	Floor	2–3 h	1–2 kg	Rating	No	No
Qualiflash	Floor/laboratory	2–3 h	1–2 kg	Rating	No	No
Prefil	Floor	2–3 h	100–1000 g	Fluidity curve	No	No
PodFA	Floor/laboratory	Days	1–2 kg	mm^2/kg	Yes	Yes
LAIS	Floor/laboratory	Days	500 g	mm^2/kg	Yes	Yes
Hot centrifuge	Laboratory	4–10 h	100–200 g	mm^2/kg	Yes	No
LiMCA	Floor	5–10 min	1.5 kg	# of particles/kg	Yes	No
Voltage probe	Floor	5–10 min	Unknown	Volume fraction	Yes	No
Ultrasound	Floor	5–10 min	Unknown	# of particles per measurement	Yes	No
X-ray radiography	Floor or laboratory	4–10 h	Almost any size	mm^2/kg	Yes	No
X-ray tomography	Laboratory	4–10 h	100–500 g	Volume fraction	Yes	No
Chemical dissolution	Laboratory	4–10 h	20–100 g	Volume fraction	Yes	No
Reduced pressure test	Floor	5–10 min	100–200 g	Rating	No	No

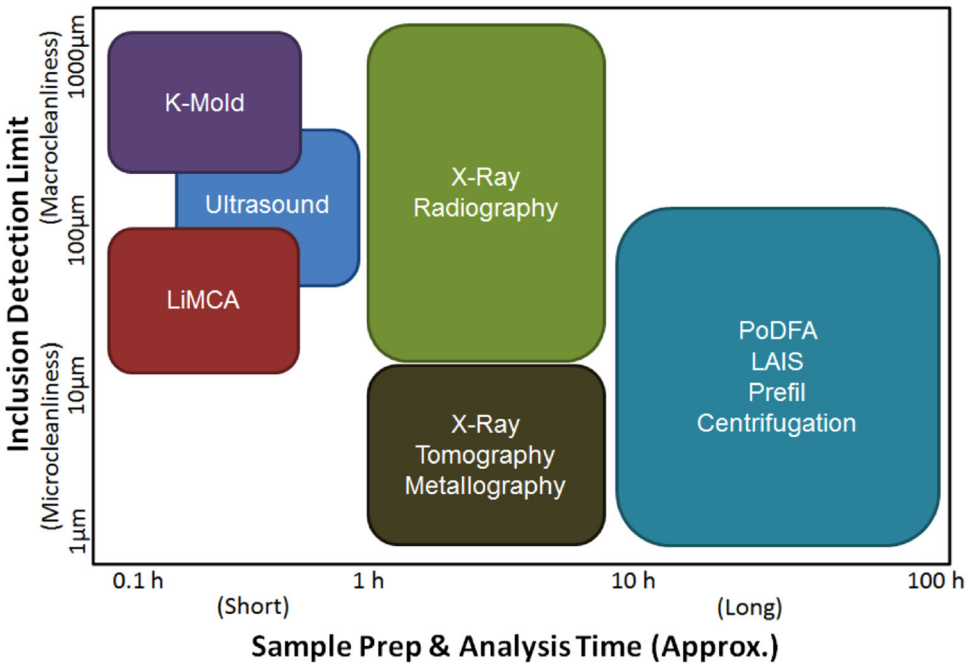

Figure 12. Qualitative comparison of inclusion detection methods with respect to inspection time and detectable range of inclusions.[10,16–18,23,32–34,42,59,62–64]

liquid metal matrix, and a magnetic field perpendicular to the current, a Lorentz force is then applied on the metal. Any non-conductive inclusions would then be forced in the opposite direction to the Lorentz force due to Newton's third law. The electrodes can be arranged to force inclusions to a free surface, where they can be measured visually. This method was able to detect particles down to 10 µm in size and take 200 samples (within a sampling

volume of 2 cm^3) per minute.[18,61] However, the surface tension of liquid aluminum prevents inclusions from breaking the melt surface. This can be addressed by pulling apart the oxide layer with rotating drums or by mechanical vibration.

Summary of Liquid Metal Inclusion Measurement Techniques

A summary of the most common methods of measuring inclusions in terms of sensing volume, type of information obtained, duration of analyses, and advantages and drawbacks is displayed in Table 2 and Figure 12. Most inclusion measurements are given in the measurement units of area per volume or kilogram of metal. Although techniques like LiMCA, ultrasound, and X-ray tomography have the capability of generating volume per volume measurements, they are cost-prohibitive and/or unable to effectively probe large quantities of melt with high enough resolution. It can be seen that no single technique is capable of describing all the information needed to assess inclusions—chemistry, concentration, and size distribution. An appropriate combination of methods is required to reach these goals. The time required of analysis, from sample gathering to measurement, can vary from a few minutes to several days. Further, there are few methods by which a large spectrum of inclusion sizes can be quickly detected.

Spectroscopy as a Tool

In situ floor methods that give an analysis of more than one facet of inclusions do not widely exist. In the metals processing field, there has been significant interest in the use of laser-induced breakdown spectroscopy (LIBS) as a tool for bulk chemistry measurement. Similar to conventional spark optical emission spectroscopy (OES), LIBS uses a short laser pulse to form a plasma on the metal surface. The elements present in the plasma emit characteristic EM radiation, which is collected and processed by a spectrograph. Because the sample interrogated is vaporized, LIBS is technically a destructive test. However, the volume sampled is on the order of 10^{-8} to 10^{-5} cm^3, which results in a very small sample size even if thousands of measurements are taken.[65] Other relevant advantages over other atomic emission techniques include: (1) LIBS can be applied to both conducting and non-conducting materials, (2) sample preparation is not necessary, (3) only an optical line of sight is required for measurement, and (4) measurements are taken in seconds.

Because only a direct line of sight is needed, LIBS is attractive for interrogating materials in extreme environments, including liquid metal. LIBS has been successfully used for monitoring dissolved elements such as C, Cr, Cu, Mn, and Ni in molten steel.[66,67] More recently, it has been applied to aluminum alloys to monitor Si, Mg, Fe, Mn, and other alloying elements.[68,69] As shown in Figure 13, developed probes for LIBS in molten metal typically use a ceramic lance with an inert gas stream to form a bubble at the end. The bubble allows for a constant, fresh surface of metal for the laser to interrogate. Fiber optic cables transmit the incoming laser pulse and outgoing light from the spark. Several probes have been developed by Rai, Lucas, and De Saro that apply this principle.[70–72] An example of one system is shown in Figure 14.

In addition to determining melt chemistry, LIBS could also be used as a means of detecting inclusions. Because of the small size of inclusions and the presence of convection in

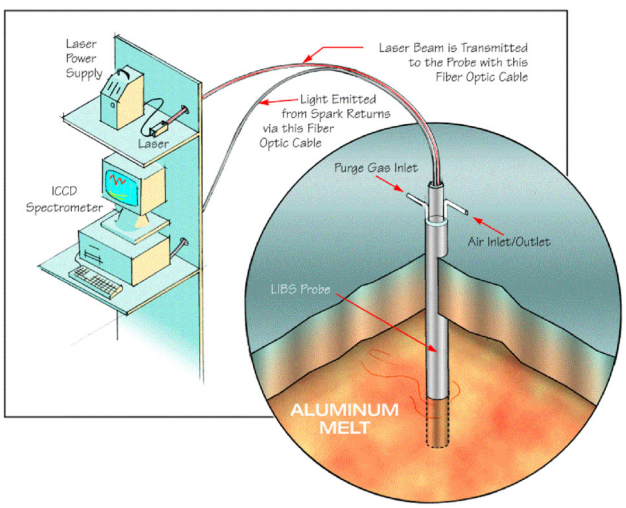

Figure 13. Schematic of LIBS for use in molten metal (Melt Cognition LLC).

Figure 14. Experimental LIBS probe (with furnace) developed by the Energy Research Company.[73]

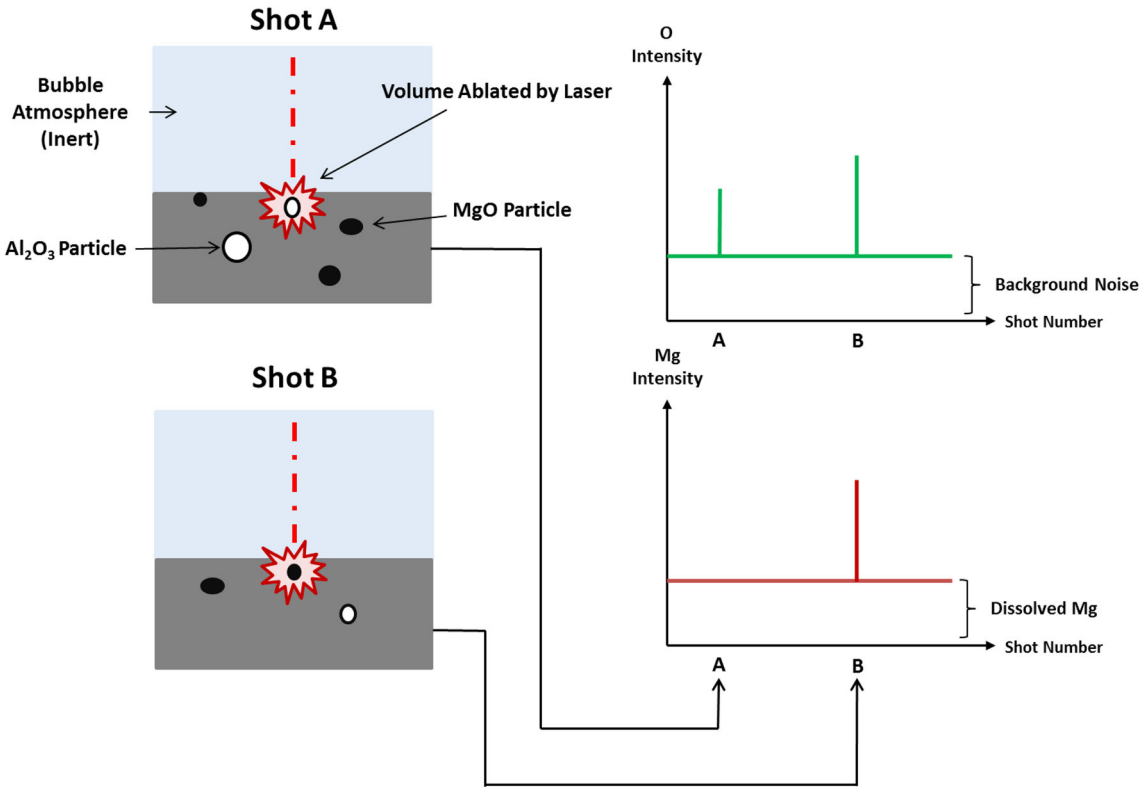

Figure 15. Example of LIBS acquisition for oxide particles in molten metal.

resistance and induction furnaces, particles are constantly moving throughout the melt. If an inclusion is present where the metal sample is vaporized, the spectrum will reveal its presence and chemistry. As illustrated in Figure 15, the oxygen peak in the spectrum will vary depending on whether an inclusion is present within the plasma. If an oxide is present, then the concentrated amount of oxygen atoms within the particle will create a spike in oxygen signal observed by the laser. In addition, if an MgO particle is ablated by the laser pulse, both a spike in Mg and O signal will be observed, allowing for differentiation between inclusions of different chemistries. In principle, the size of the elemental intensity spike from a particle "hit," is proportional to the size of the particle. A large oxide inclusion would emit a higher oxygen signal than a small inclusion.

Similar work has been done on determining the presence and chemistry of inclusions in solid steel samples via statistical evaluation with OES.[74–78] In work done by Pande et al., OES with pulse discrimination analysis was used to assess the concentration of Al_2O_3 inclusions in ultralow carbon steels. They found that an aluminum-containing particle with yield significantly higher Al signal than the bulk metal. Signal from dissolved Al will follow a Gaussian distribution, while signals contributing to particles fall out of the distribution. Sabsabi et al. have found similar results on magnesium alloys and were able to achieve elemental mapping on solid samples.[79] No work to date has been performed on aluminum.

In molten metal, particles are attracted to free surfaces due to their high surface-to-volume ratio and poor wettability. Because the LIBS probe forms a free surface through a bubble of inert gas, inclusions may naturally gravitate toward it. Hudson et al. examined the possibility of using LIBS to sense inclusions in liquid aluminum. By bubbling air into liquid Al and subsequently adding clean metal, it was found that oxygen intensity varied with metal cleanliness (Figure 16). Thus, it was concluded that, to a first order, LIBS could differentiate between relatively clean and dirty metal.[73] In similar experiments with SiC particles in molten pure aluminum, a linear relationship was observed between average Si signal and SiC volume fractions of less than 0.006 % (Figure 17). This is similar to typical concentrations of oxide inclusions.[80]

Because of the discrete nature of inclusions in the melt, parameters such as average particle concentration, size distribution, laser repetition rate, and sampling volume must be taken into account. Sampling statistics must be considered to answer such questions as: (1) How many particles must be sampled to determine a representative measurement and (2) can accurate inclusion concentration values be determined with relatively clean aluminum (<1 ppm)?

Hahn and colleagues have carried out extensive work on the nature of LIBS sampling for discrete nanoparticles in aerosols. By knowing the sampling volume as well as the concentration of the element in the particle, Hahn derived that the overall particle size can be expressed as:

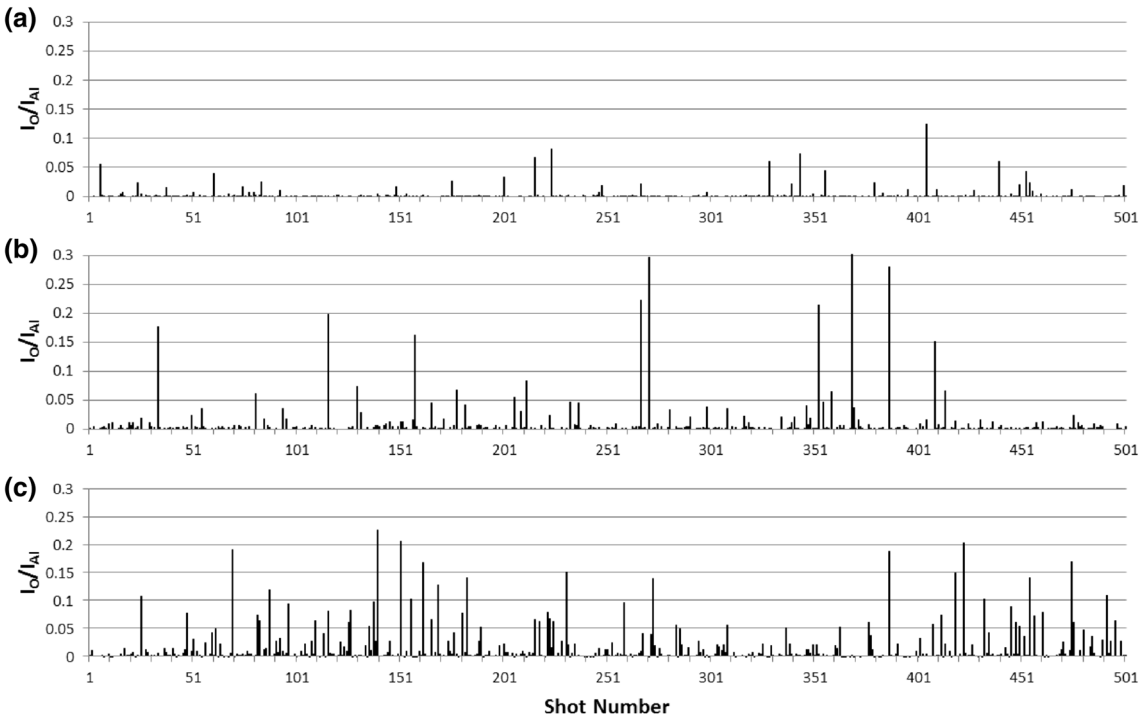

Figure 16. Variance in oxygen intensity versus LIBS measurement number for: (a) reference clean metal, (b) half clean, half dirty, and (c) reference dirty metal.[73]

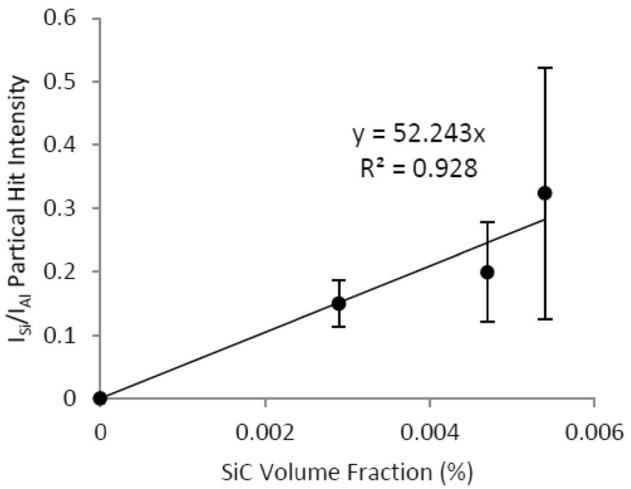

Figure 17. Signal from SiC particle hits versus volume fraction. Error bars represent standard deviation.[80]

$$d = \left(\frac{6C_i V_s}{\pi \rho f}\right)^{1/3} \qquad \text{Eqn. 7}$$

Here, "C_i" is the equivalent mass concentration of the particle and "f" is the mass fraction of the elemental signal with respect to the overall inclusion mass, "V_s" is the effective sampling volume, and "ρ" is the particle density. For a homogeneous particle (an Fe particle, for example), "f" is equal to one. In experiments done with metal particles in gas streams, it was determined that at least 20 particle hits were required to obtain a representative measure of the particle concentration and size distribution. Successful LIBS measurements of CaO particles in aerosol streams were achieved for concentrations of <1 ppm.[81–84] Therefore, in principle, the particle size of inclusions can be determined by calculating the concentration of oxygen signal in each laser measurement.

Conclusion

The drive to achieve cleanliness in aluminum and its alloys had resulted in a plethora of techniques focused on assessing and quantifying the number of inclusions present. The state of the art with respect to inclusion detection in aluminum and its alloys has been reviewed. These methods include:

- Optical microscopy
- Ultrasound (solid and liquid state)
- X-ray radiography and tomography
- Electromagnetic sensing
- Fracture tests
- Reduced pressure tests
- Filtration and centrifugation
- Chemical dissolution

The key limitation with current methods is that they are unable to quickly determine chemistry, concentration, and size distribution of inclusions within the molten metal. The concept of using in situ laser-induced breakdown spectroscopy (LIBS) as a means of detecting and quantifying

inclusions has been presented. Ongoing experiments have shown that this new technique shows promise, but more research is required to analyze multi-element inclusions, determine optimal sampling schemes, and develop proper procedures for calculating particle size from concentration.

REFERENCES

1. S. Shivkumar, L. Wang, D. Apelian, Molten-metal processing of advanced cast-aluminum alloys. JOM **43**(1), 26–32 (1991)
2. S. Rawal, Metal-matrix composites for space applications. JOM **53**(4), 14–17 (2001)
3. M.M. Makhlouf, Aluminum melt preparation for high integrity die castings. Die Cast. Eng. **52**(6), 18–23 (2008)
4. S.T. Johansen, S. Gradahl, O. Dahle, I.R. Johansen, in *Light Metals 1996*, ed. by W. Hale (TMS, Warrendale, PA, 1996), pp. 1027–1031
5. J. Campbell, The origin of Griffith cracks. Metall. Mater. Trans. B **42**(6), 1091–1097 (2011)
6. P. Pouly, E. Wuilloud, in *Light Metals 1997*, ed. by R. Huglen (TMS, Warrendale, PA, 1997), pp. 829–835
7. P.N. Crepeau, Molten aluminum contamination: gas, inclusions, and dross. Mod. Cast. **87**(7), 39–41 (1997)
8. C.J. Siemensen, G. Berg, A survey of inclusions in aluminum. Aluminum **56**, 340–355 (1980)
9. J. Campbell, *Castings*, 2nd edn. (Butterworth-Heinemann, Jordan Hill, 2003)
10. D. Doutre, B. Gariepy, J.P. Martin, G. Dube, in *Essential Readings in Light Metals*, vol. 3, ed. by J.F. Granfield, D.G. Eskin (Wiley, Hoboken, NJ, 2013), pp. 1179–1195
11. J. Campbell, Stop pouring, start casting. Int. J. Metalcast. **6**(3), 7–18 (2012)
12. K. Hoshino, T. Nishizaka, K. Kakimoto, T. Yoshida, in *Light Metals 1996*, ed. by W. Hale (TMS, Warrendale, PA, 1996), pp. 833–838
13. H.P. Krug, W. Schneider, in *Light Metals 1998*, ed. by B. Welch (TMS, Warrendale, PA, 1998), pp. 863–870
14. X. Wang, in *Light Metals 1997*, ed. by R. Huglen (TMS, Warrendale, PA, 1997), pp. 963–972
15. P. Bakke, J.A. Laurin, A. Provost, D.O. Karlsen, in *Light Metals 1997*, ed. by R. Huglen (TMS, Warrendale, PA, 1997), pp. 1019–1026
16. C.J. Siemensen, Sedimentation analysis of inclusions in aluminum and magnesium. Metall. Trans. B Process Metall. **12**(4), 733–743 (1981)
17. C.J. Siemensen, G. Strand, Analysis of inclusions in aluminum by dissolution of the samples in hydrochloric nitric-acid. Fresenius Z. Fur Anal. Chem. **308**(1), 11–16 (1981)
18. S. Makarov, D. Apelian, R. Ludwig, in *Transactions of the One Hundred Third Annual Meeting of the American Foundrymen's Society* (AFS, Schaumburg, Il, 1998), pp. 727–735
19. T. Gudmundsson, G. Saevarsdottir, T.I. Sigfusson, D.G. McCartney, in *Light Metals 1997*, ed. by R. Huglen (TMS, Warrendale, PA, 1997), pp. 851–855
20. L. Liu, F.H. Samuel, Effect of inclusions on the tensile properties of Al–7% Si–0.35% Mg (A356.2) aluminium casting alloy. J. Mater. Sci. **33**(9), 2269–2281 (1998)
21. D. Dispinar, C. Kahruman, J. Campbell, *Shape Casting: 5th International Symposium* (2014). doi: 10.1002/9781118888100.ch21
22. J.G. Kaufman, E.L. Rooy, *The Influence and Control of Porosity and Inclusions in Aluminum Castings, Aluminum Alloy Castings: Properties, Processes, and Applications* (ASM International, Materials Park, OH, 2004)
23. H.V. Atkinson, G. Shi, Characterization of inclusions in clean steels: a review including the statistics of extremes methods. Prog. Mater Sci. **48**(5), 457–520 (2003)
24. P.S. Mohanty, F.H. Samuel, J.E. Gruzleski, in *Transactions of the 99th Meeting of the American Foundrymen's Society* (AFS, Schaumburg, Il, 1995), pp. 555–564
25. P.S. Mohanty, F.H. Samuel, J.E. Gruzleski, in *Proceedings of the International Symposium on Light Metals Processing and Applications*, ed. by C. Bickert (Canadian Institute of Mining, Metallurgy, and Petroleum, Montreal, 1993), pp. 272–282.
26. M. Di Sabatino, L. Arnberg, S. Rørvik, A. Prestmo, The influence of oxide inclusions on the fluidity of Al–7 wt% Si alloy. Mater. Sci. Eng., A **413–414**, 272–276 (2005)
27. Y.D. Kwon, Z.H. Lee, The effect of grain refining and oxide inclusion on the fluidity of Al–4.5 Cu–0.6 Mn and A356 alloys. Mater. Sci. Eng., A **360**(1–2), 372–376 (2003)
28. T.L. Buijs, D. Gagnon, C. Dupuis, in *Light Metals* (2014). doi:10.1002/9781118888438.ch169
29. ASTM International, E45-13, Standard test methods for determining the inclusion content of steel, (West Conshohocken, PA, 2013)
30. R. Fritzsch, J.Y. Hwang, C. Bai, J. Carpenter, S.J. Ikhmayies, in *Characterization of Minerals, Metals, and Materials 2013* (Wiley, New York, 2013), pp. 67–77
31. P.J. Wray, O. Richmond, H.L. Morrison, Use of the Dirichlet tessellation for characterizing and modeling nonregular dispersions of second-phase particles. Metallography **16**(1), 39–58 (1983)
32. S. Poynton, M. Brandt, J. Grandfield, in *Essential Readings in Light Metals*, vol. 3, ed. by J.F. Granfield, D.G. Eskin (Wiley, Hoboken, NJ, 2013), pp. 1179–1195
33. M.B. Djurdevic, Z. Odanovic, J. Pavlovic-Krstic, Melt quality control at aluminum casting plants. Metall. Mater. Eng. **16**(1), 63–76 (2010)

34. D. Neff, in *Proceedings of the North American Die Casting Association Congress* (NADCA, Arlington Heights, Il, 2002)
35. E.W.J. Miller, M.P. Stephenson, J. Beech, A technique for the direct observation of alloy solidification. J. Phys. E Sci. Instrum. **8**(1), 33 (1975)
36. Anonymous, *Digital radiography for aluminum castings*, in *Foundry Management and Technology* (Penton Media, Inc., Cleveland, 2006), p. 15
37. O. Lashkari, L. Yao, S. Cockcroft, D. Maijer, X-ray microtomographic characterization of porosity in aluminum alloy A356. Metall. Mater. Trans. A **40**(4), 991–999 (2009)
38. R.G. Maev, J.H. Sokolowski, H.T. Lee, E.Y. Maeva, A.A. Denissov, Bulk and subsurface structure analysis of the 319 aluminum casting using acoustic microscopy methods. Mater. Charact. **46**(4), 263–269 (2001)
39. F. Silva, J.J. Williams, B.R. Müller, M.P. Hentschel, N. Chawla, Three-dimensional microstructure visualization of porosity and Fe-rich inclusions in SiC particle-reinforced Al alloy matrix composites by X-ray synchrotron tomography. Metall. Mater. Trans. A **41**(8), 2121–2128 (2010)
40. T. Kundu, *Ultrasonic Nondestructive Evaluation: Engineering and Biological Material Characterization* (CRC Press, Boca Raton, 2003)
41. T.L. Mansfield, Ultrasonic technology for measuring molten aluminum quality. J. Met. **34**(9), 54–57 (1982)
42. R. Guthrie, M. Isac, In-situ sensors for liquid metal quality. High Temp. Mater. Process. **31**(4–5), 633–643 (2012)
43. R.S. Young, D.E. Pitcher, *Methods of and apparatus for testing molten metal*, US Patent 3444726 (1969)
44. M. Kurban, I.D. Sommerville, N.D.G. Mountford, P.H. Mountford, in *Light Metals 2005*, ed. by H. Kvande (TMS, Warrendale, PA, 2005), pp. 945–949
45. MetalVision Manufacturing Company Ltd, *Offline Crucible Testing and Comparison with PoDFA® Data*. http://metalvision.ca/comparison.html. Accessed 28 July 2015
46. Y. Ono, J.F. Moisan, C.K. Jen, Ultrasonic techniques for imaging and measurements in molten aluminum. IEEE Trans. Ultrason. Ferroelectr. Freq. Control **50**(12), 1711–1721 (2003)
47. P.G. Enright, I.R. Hughes, A shop floor technique for quantitative measurement of molten metal cleanliness of aluminium alloys. Foundryman (UK) **89**(11), 390–395 (1996)
48. D. Apelian, in *Proceedings of the 3rd International Conference on Molten Aluminum Processing* (AFS, Schaumburg, Il, 1992), pp. 1–15
49. S.A. Levy, in *Light Metals 1981*, ed. by C.J. McMinn, E.M. Adkins, J.E. Andersen (Metallurgical Society of AIME, 1981), pp. 723–733
50. D. Sampath, P.G.J. Flick, J. Pool, W. Boender, W. Van Rijswik, in *Light Metals 1996*, ed. by W. Hale (TMS, Warrendale, PA, 1996), pp. 817–821
51. D. Apelian, M. Makhlouf, *High Integrity Aluminum Die Castings: Alloys, Processes, and Melt Preparation* (NADCA, Wheeling, Il, 2006), pp. 118–119
52. F.R. Mollard, J.E. Dore, W.S. Peterson, in *Light Metals 1972,* ed. by W.C. Rotsell (Metallurgical Society of AIME, 1972), pp. 483–501
53. M. Iwatsuki, S. Nishida, T. Kitamura, Determination of inclusions in molten aluminum alloy by X-ray diffractometry after selective dissolution. Anal. Sci. **14**(3), 617–619 (1998)
54. R.I.L. Guthrie, D.A. Doutre, in *International Seminar on Refining and Alloying of Liquid Aluminum and Ferro-Alloys*, ed. by T.A. Engh, S. Lyng, H.A. Oye (Trondheim, 1985), pp. 147–163
55. M. Badowski, M. Gokelma, J. Morscheiser, T. Dang, P. Le Brun, S. Tewes, in *Light Metals* (2015). doi: 10.1002/9781119093435.ch162
56. D. Apelian, M. Makhlouf, Quality assurance methods, *High Integrity Aluminum Die Castings: Alloys, Processes, and Melt Preparation* (North American Die Casting Association, Wheeling, 2006)
57. W.M. Rasmussen, To pour or not to pour—the dilemma of assessing your aluminum melt's cleanliness. Mod. Cast. **86**(2), 45–48 (1996)
58. S. Dasgupta, L. Parmenter, D. Apelian, in *Proceedings of the 5th International Molten Metal Conference* (AFS, Schaumburg, Il, 1998), pp. 285–300
59. L. Parmenter, D. Apelian, F. Jensen, Development of a statistically optimized test method for the reduced pressure test. Trans. Am. Foundrym. Soc. **106**(106), 439–452 (1998)
60. S. Makarov, R. Ludwig, D. Apelian, Identification of depth and size of subsurface defects by a multiple-voltage probe sensor: analytical and neural network techniques. J. Nondestr. Eval. **19**(2), 67 (2000)
61. S. Makarov, R. Ludwig, D. Apelian, Electromagnetic visualization technique for non-metallic inclusions in a melt. Meas. Sci. Technol. **10**(11), 1047–1053 (1999)
62. M.A. Dewan, M.A. Rhamdhani, J.B. Mitchell, C.J. Davidson, G.A. Brooks, M. Easton, J.F. Grandfield, Control and removal of impurities from Al melts: a review. Mater. Sci. Forum **693**, 149–160 (2011)
63. T.A. Utigard, I.D., in *Light Metals 2005*, ed. H. Kvande (TMS, Warrendale, PA, 2005), pp. 951–986
64. ASTM International, E155-25, Standard reference radiographs for inspection of aluminum and magnesium castings, (West Conshohocken, PA, 2015)
65. D.W. Hahn, N. Omenetto, Laser-induced breakdown spectroscopy (LIBS), Part I: review of basic diagnostics and plasma-particle interactions: still-challenging issues within the analytical plasma community. Appl. Spectrosc. **64**(12), 335A–366A (2010)
66. D.A. Cremers, F. L. Archuleta, H.C. Dilworth, Rapid analysis of steels using laser-based techniques, in *5th Process Technology Conference on Measurement and*

Control Instrumentation in the Iron and Steel Industry (AIST, Detroit, 1985)
67. R. Noll, H. Bette, A. Brysch, M. Kraushaar, I. Mönch, L. Peter, V. Sturm, Laser-induced breakdown spectrometry—applications for production control and quality assurance in the steel industry. Spectrochim. Acta Part B Atomic Spectrosc. **56**(6), 637–649 (2001)
68. M. Sabsabi, P. Cielo, Quantitative-analysis of aluminum-alloys by laser-induced breakdown spectroscopy and plasma characterization. Appl. Spectrosc. **49**(4), 499–507 (1995)
69. R. De Saro, A. Weisberg, J. Craparo, in *Light Metals 2003*, ed. by P.N. Crepeau (TMS, Warrendale, PA, 2003), pp. 1103–1107
70. A.K. Rai, F.Y. Yueh, J.P. Singh, H. Zhang, High temperature fiber optic laser-induced breakdown spectroscopy sensor for analysis of molten alloy constituents. Rev. Sci. Instrum. **73**(10), 3589–3599 (2002)
71. J.M. Lucas, M. Sabsabi, R. Heon, *Method and apparatus for molten material analysis by laser induced breakdown spectroscopy*, US Patent 6909505B2 (2003)
72. R. De Saro, A. Weisberg, *Apparatus and method for in situ, real time measurements of properties of liquids*, US Patent 20030197125A1 (2003)
73. S.W. Hudson, D. Apelian, in *Light Metals* (2014). doi: 10.1002/9781118888438.ch170
74. H. Falk, P. Wintjens, Statistical evaluation of single sparks. Spectrochim. Acta Part B Atomic Spectrosc. **53**(1), 49–62 (1998)
75. H.-M. Kuss, H. Mittelstaedt, G. Mueller, Inclusion mapping and estimation of inclusion contents in ferrous materials by fast scanning laser-induced optical emission spectrometry. J. Anal. Atomic Spectrom. **20**(8), 730–735 (2005)
76. H.M. Kuss, S. Lungen, G. Muller, U. Thurmann, Comparison of spark OES methods for analysis of inclusions in iron base matters. Anal. Bioanal. Chem. **374**(7–8), 1242–1249 (2002)
77. F. RubyMeyer, G. Willay, Rapid identification of inclusions in steel by OES-CDI technique. Rev. Metall. Cah. D Inf. Tech. **94**(3), 367 (1997)
78. M.M. Pande, M.X. Gu, R. Dumarey, S. Devisscher, B. Blanpain, Determination of steel cleanliness in ultra low carbon steel by pulse discrimination analysis-optical emission spectroscopy technique. ISIJ Int. **51**(11), 1778–1787 (2011)
79. M. Sabsabi, L. St-Onge, V. Detalle, J.M. Lucas, Laser-induced breakdown spectroscopy: a new tool for process control, in *16th World Conference on Non-Destructive Testing* (Canadian Institute for NDE, Hamilton, Ontario, 2004)
80. S.W. Hudson, J. Craparo, R. De Saro, D. Apelian, in *Light Metals* (2015). doi: 10.1002/9781119093435.ch166
81. D.W. Hahn, W.L. Flower, K.R. Hencken, Discrete particle detection and metal emissions monitoring using laser-induced breakdown spectroscopy. Appl. Spectrosc. **51**(12), 1836–1844 (1997)
82. D.W. Hahn, Laser-induced breakdown spectroscopy for sizing and elemental analysis of discrete aerosol particles. Appl. Phys. Lett. **72**(23), 2960–2962 (1998)
83. D.W. Hahn, M.M. Lunden, Detection and analysis of aerosol particles by laser-induced breakdown spectroscopy. Aerosol Sci. Technol. **33**(1–2), 30–48 (2000)
84. P.K. Diwakar, K.H. Loper, A.M. Matiaske, D.W. Hahn, Laser-induced breakdown spectroscopy for analysis of micro and nanoparticles. J. Anal. Atomic Spectrom. **27**(7), 1110–1119 (2012)